

# EXPERIMENTAL STABILITY MAPS FOR A BWR-TYPE SMALL MODULAR REACTOR

**S. Shi, Y.-C. Lin, W. S. Yang**

School of Nuclear Engineering, Purdue University  
400 Central Drive, West Lafayette, IN 47907, USA  
shi67@purdue.edu; lin298@purdue.edu; yang494@purdue.edu

**M. Ishii**

Department of Nuclear Engineering  
Purdue University  
400 Central Drive, West Lafayette, IN 47907, USA  
ishii@purdue.edu

## ABSTRACT

The Purdue NMR (Novel Modular Reactor) is a small modular reactor (SMR) based on boiling water reactor (BWR) technologies and natural circulation cooling during normal operation and accident conditions. Under natural circulation conditions, a two-phase coolant flow may become unstable and lead to significant control and safety problems in nuclear power plants. In order to study the thermal-hydraulic flow instability phenomena and obtain the stability boundary at low pressure conditions, the quasi-steady tests were performed following startup transient tests in a well-scaled BWR-type test facility based on sound scaling methodology developed for the design of Purdue University Multi-Dimensional Integral Test Assembly for the GE SBWR. The test facility can be operated under a pressure from 50 kPa to 1000 kPa and is installed with a pressurizer for the quasi-steady state tests. The effects of system pressure and void reactivity feedback are investigated on the flow instability map for the NMR. During the quasi-steady tests, the core inlet subcooling and heat flux of the test facility are controlled to obtain the stable and unstable operating conditions under constant system pressure. With the inlet subcooling changing from high subcooling to low subcooling, the flow develops from single-phase natural circulation to two-phase natural circulation. The experimental stability maps in dimensionless plane ( $N_{zu}$ - $N_{sub}$ ) clearly show the boundary of the flashing instability observed in previous startup transient tests. The flashing instability occurring in the chimney section at lower pressure is a thermal non-equilibrium phenomenon because the boundary is located above the zero-quality line at the core exit. In addition, the flashing stability boundary moves to the zero-quality line at the core exit as system pressure increases over 400 kPa. The void reactivity feedback mechanism does not show significant effects on the stability boundary except cause some power oscillations in single-phase region.

## KEYWORDS

Natural circulation NMR, Flow instability, Quasi-steady state tests, Stability maps

## 1. INTRODUCTION

Categorized as generation III/III+ nuclear reactors, the design of small modular reactor (SMR) is receiving much more attention after nuclear accidents in Fukushima. Compared to traditional nuclear reactors, SMR designs offer advantages of siting flexibility, scalability, and inherent passive safety, etc. The Purdue NMR (Novel Modular Reactor), which is developed based on GE SBWR-600 [1] at Purdue University, is a BWR-type natural circulation small modular reactor. The NMR with an electricity output of 50 MWe (NMR-50) [2] is about one third height and area of a conventional boiling water reactor. The fuel cycle length of the NMR-50 is extended to 10 years by using AREVA Atrium-10B fuel assembly design recently. The engineering safety system design of NMR-50 includes a two-layer passive safety system for adequate removal of decay heat for an indefinite period without outside intervention.

The design of natural circulation reactor including NMR-50 can have flow instability issues during the startup transients and low pressure conditions due to the existence of chimney section above the core. Flashing instability and density wave oscillation are the two main flow instabilities observed from previous startup experiments [3]. Figure 1 shows the time trace of natural circulation rate for one startup transients. The flashing instability, which can be seen from 50 minutes to 150 minutes, is caused by the vapor generation in the chimney due to reduced hydrostatic head at low pressure conditions. Then sudden increased void fraction in the chimney enhances the driving force of natural circulation and therefore increases the mass flow rate, which might pose a significant challenge in two-phase natural circulation systems. Flashing instability usually occurs at low pressure during the transition phase between the single-phase natural circulation and the two-phase natural circulation. The density wave oscillations were observed at the beginning of the two-phase natural circulation while diminished with increasing power density and system pressure during the startup transients.

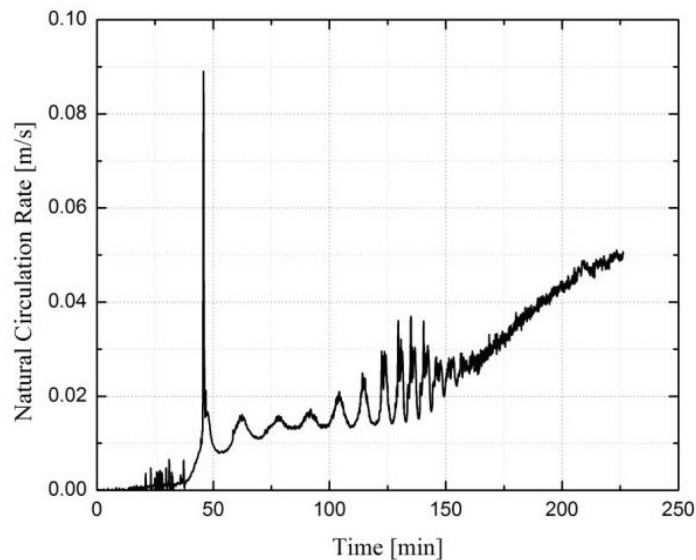


**Figure 1. Natural Circulation Rate for the Slow Normal Startup Transients.**

The purpose of this paper is to obtain experimental stability maps by performing quasi-steady tests on a well-scaled test facility at low pressure conditions. The system pressure, core heat flux, and void reactivity feedback are investigated on the stability plane for the NMR-50. Section 2 describes the stability plane commonly used in flow stability analysis. Section 3 shows the test facility design and instrumentation. Section 4 presents experimental results and analyses. And the key conclusions of this research are summarized in Section 5.

## 2. STABILITY PLANE

The stability plane was firstly applied by Ishii [4] to determine the stability boundary for the density wave oscillations in a heated system using perturbation method. Now it is widely accepted as a standard tool to analyze different flow instabilities. The stability map is plotted in the plane of dimensionless subcooling number and phase change number (Zuber Number), which are defined as follows.

$$N_{pch} = \frac{\dot{Q}}{\dot{m}_o} \frac{\Delta\rho}{\rho_g \Delta i_{fg}} \propto \frac{\text{core enthalpy rise}}{\text{latent heat}} \quad (1)$$

$$N_{sub} = \Delta i_{sub} \frac{\Delta\rho}{\rho_g \Delta i_{fg}} \propto \frac{\text{core inlet subcooling}}{\text{latent heat}} \quad (2)$$

where  $\dot{Q}$  and  $\dot{m}_o$  identify the total heat transfer rate and coolant flow rate in the heated section, respectively. Other symbols in the above set of equations conform to standard nomenclature. From the non-dimensionalized steady-state energy equation, the subcooling and heat input to the system can have the relations as

$$N_{pch} - N_{sub} = x_e \frac{\Delta\rho}{\rho_g} \quad (3)$$

where  $x_e$  denotes the core exit quality. And the length of non-boiling region is given by

$$\lambda^* = \frac{N_{sub}}{N_{pch}} \quad (4)$$

The basic characteristics of the stability plane in Eq. (3) are illustrated in Fig. 2.

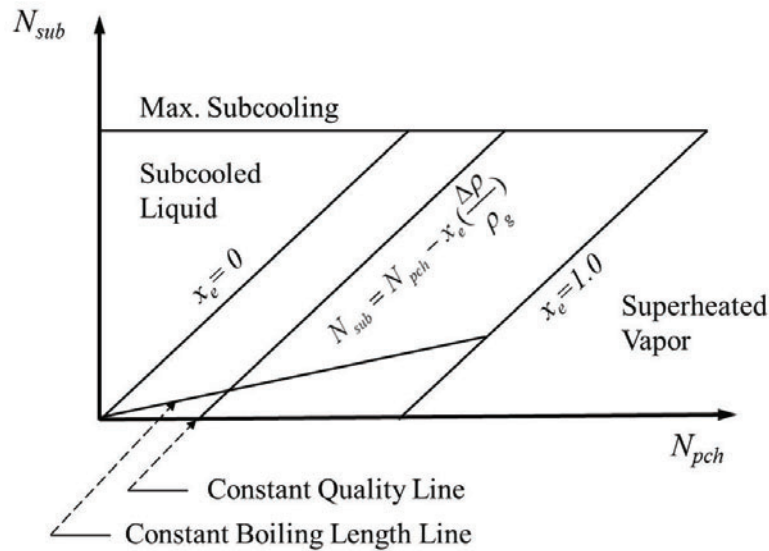


Figure 2. Stability Plane [4].

### 3. EXPERIMENTAL APPROACHES

#### 3.1. Test Facility Configuration

The important thermal-hydraulic parameters, i.e., system pressure, power level, and core inlet temperature, needs to be controlled during the quasi-steady tests to obtain the experimental stability maps at different flow conditions. The quasi-steady state test facility is similar to that for the study of flow instability for the startup transients, which was scaled down from the NMR-50 based on the three-level scaling methodology [5]. The scaling analyses and verifications were summarized in previous research on flow instability [3]. The detailed schematics of the facilities for the quasi-steady tests are shown in Fig.3. The main design parameters for the test facility are given in Table I. The geometry of the test facility is determined based on a previous design of a simulated reactor core [6]. The elevation of this test facility is close to that of the prototype (NMR-50). The test facility is composed of core section, riser (chimney), separator, and downcomer section. In addition, this test facility has another three-phase 18 kW preheater installed at the upstream of the core inlet and another pipe subcooler in the upper downcomer section. The designs of preheater and pipe subcooler are used to set the inlet subcooling for certain conditions during the quasi-steady tests.

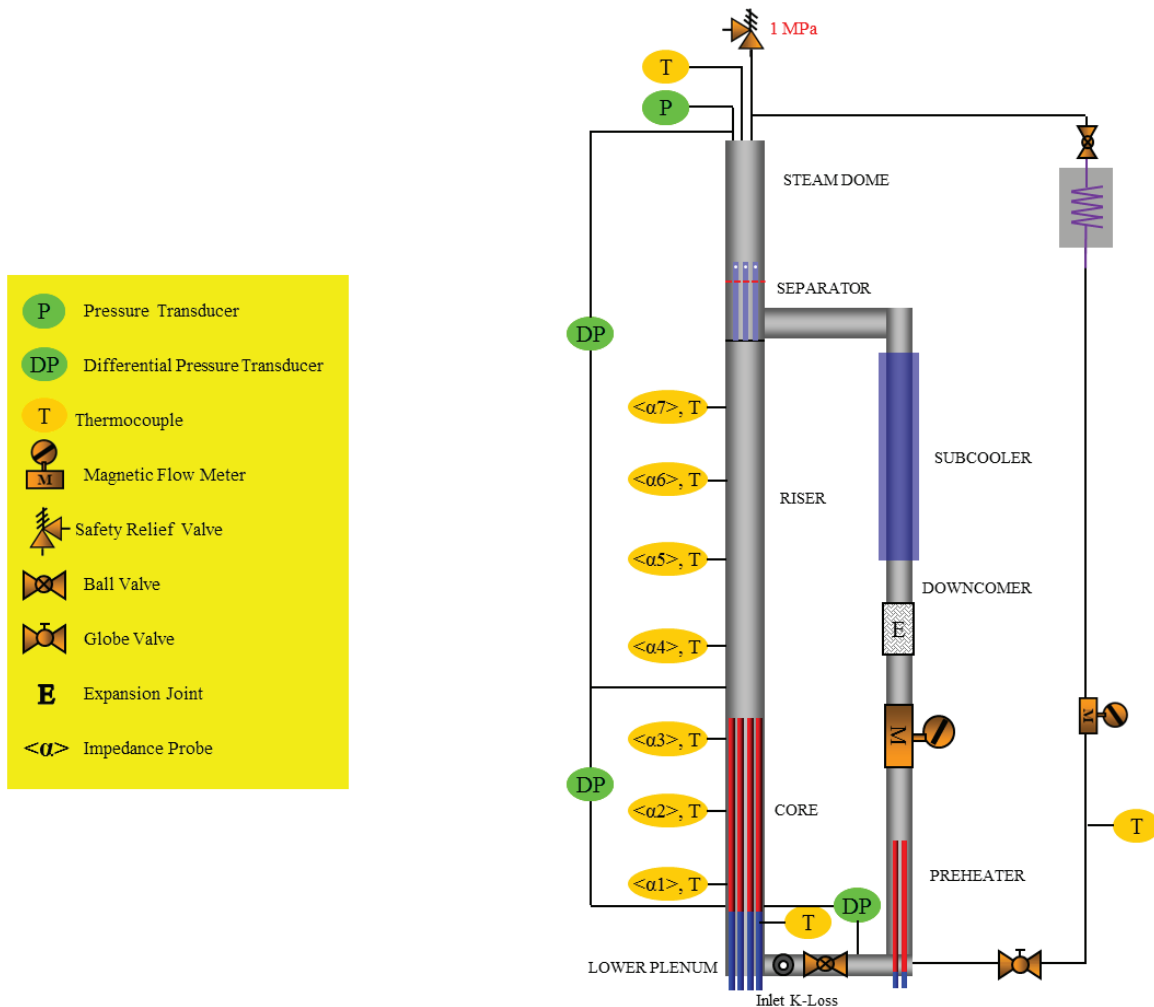


Figure 3. Schematic of the Steady State Facility.

**Table I. Geometrical design parameters of the test facility**

<b>Component</b>	<b>Specification</b>	<b>Test Facility</b>
<b>RPV</b>	Total height (mm)	7000
	Wall materials	304 Stainless steel
	Wall thickness (mm)	3.0
	TAF elevation (mm)	1950
	Top of chimney (mm)	5260
	Top of separator tubes (mm)	5950
<b>Core</b>	Active fuel length (mm)	1130
	Hydraulic diameter (mm)	23.0
	Inner diameter (mm)	82.8
	Wall thickness (mm)	3.05
<b>Chimney</b>	Inner diameter (mm)	82.8
	Wall thickness (mm)	3.05
<b>Downcomer</b>	Inner diameter (mm)	54.8
	Wall thickness (mm)	2.77
<b>Subcooler</b>	Height (mm)	1700
	Inner diameter (mm)	82.8

### 3.2. Test Instrumentation

This test facility is equipped with Honeywell pressure transducers, T-type thermocouples, and Honeywell magnetic flow meters to measure different thermal-hydraulic parameters. The steam dome pressure and core inlet pressure can be obtained through two absolute pressure transducers. Three differential pressure transducers measure the pressure drops at different locations in Fig. 3. Temperatures measured by thermocouples can be used to determine the saturated condition with pressure. The single phase flow velocity at the core inlet, which is defined as the loop natural circulation rate, can be measured from the magnetic flow meter installed in the downcomer section.

The impedance void meter is a key instrument for void fraction measurements. It can provide the void fraction by measuring the electrical impedance of two-phase flow. The home-made impedance void meter consists of two major components: a probe and an electronic circuit. For good mechanical and noncorrosive properties, stainless steel is chosen as the material for the electrodes. Teflon is used as an electrical insulator between electrodes, and between the electrodes and outer shell of the probe. There are two types of impedance void meter used in the current facility. One design in the heated section (core part) uses four heater rods with one stainless steel ring and the partition as electrodes as shown in Fig. 4. Another design for the unheated section (chimney part) uses two stainless steel rings as electrodes as shown in Fig. 5. The two rings are mounted inside the wall and insulated from each other. There are three impedance probes (IMP01-IMP03) in the core part, and four probes (IMP04-IMP07) in the chimney part. The accuracy of IMP can reach 0.5 % in absolute value for low void fraction measurement based on the calibration [3].

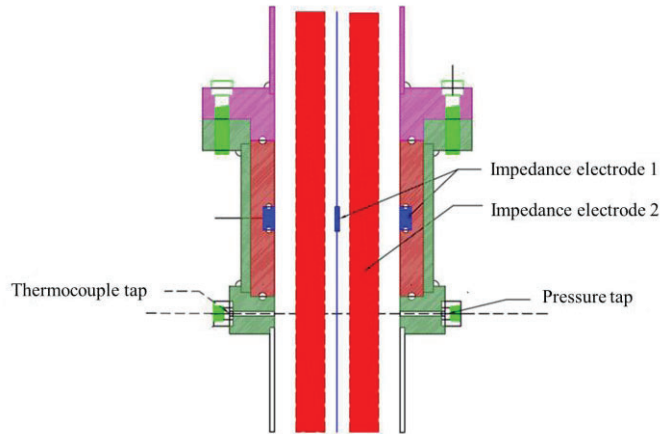


**Figure 4. Instrumentation Ports on the Heated Section.**

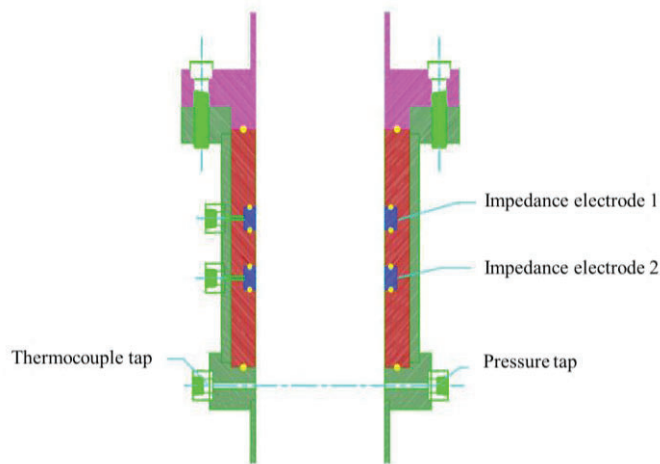


**Figure 5. Instrumentation Ports on the Chimney Section.**

### 3.3. Stability Criteria

The time trace signals of thermal-hydraulic parameters obtained during the quasi-steady tests can be used to determine if the system is stable or not. For example, the core inlet velocity is analyzed with the void fraction signals at the top of the chimney for the flashing instability. The mean core inlet velocity and the statistical root mean squared error (RMSE) are defined as follows:

$$\bar{v}_{in} = \frac{1}{n} \sum_{i=1}^n v_{in,i} \quad (5)$$

$$v_{in,RMSE} = \sqrt{\frac{\sum_{i=1}^n (v_{in,i} - \bar{v}_{in})^2}{n}} \quad (6)$$

Two criteria are used to classify the experimental conditions into unstable and stable condition.

1. Flow is stable if the RMSE of the inlet flow velocity is less than 10 % of the mean inlet flow velocity.
2. The unstable boundary can be determined if the amplitude of the flow oscillation starts increasing exponentially rather than keep constant in stable region.

#### 4. TEST RESULTS

Before the quasi-steady tests, the degassing procedure is needed to remove all the non-condensable gas inside. After setting up initial pressure and water level, the quasi-steady test starts from high subcooling number to low subcooling number for a fixed heat flux by manipulating pipe subcooler and preheater. This process is then repeated for different core heat flux by increasing core power output. In the quasi-steady tests, the inlet subcooling number is directly determined by the core inlet temperature and core inlet pressure. And the phase change number is determined by both core heat flux and mass flow rate for the natural circulation boiling water reactor, which is quite different from the forced circulation reactor. The experimental test results are presented in the following sections.

##### 4.1. Stability Maps at 200 kPa of System Pressure

The quasi-steady tests were initially performed to obtain the stability map at 200 kPa. The experimental testing points are firstly plotted in the plane of core heat flux and inlet subcooling in Fig. 6. It shows that the testing conditions go from stable single-phase natural circulation to stable two-phase natural circulation as the inlet subcooling decreases for a fixed heat flux. The stable test conditions are marked by blue square points for both single-phase and two-phase regions. Between two stable phases, the flashing induced intermittent oscillations, which are marked by red color, occur at the top of the chimney. Two stability boundaries are drawn between the stable and unstable conditions. The first boundary between the single-phase natural circulation and the transition phase is close to a straight line. However, the second boundary between the transition phase and the two-phase natural circulation shows non-linear characteristic.

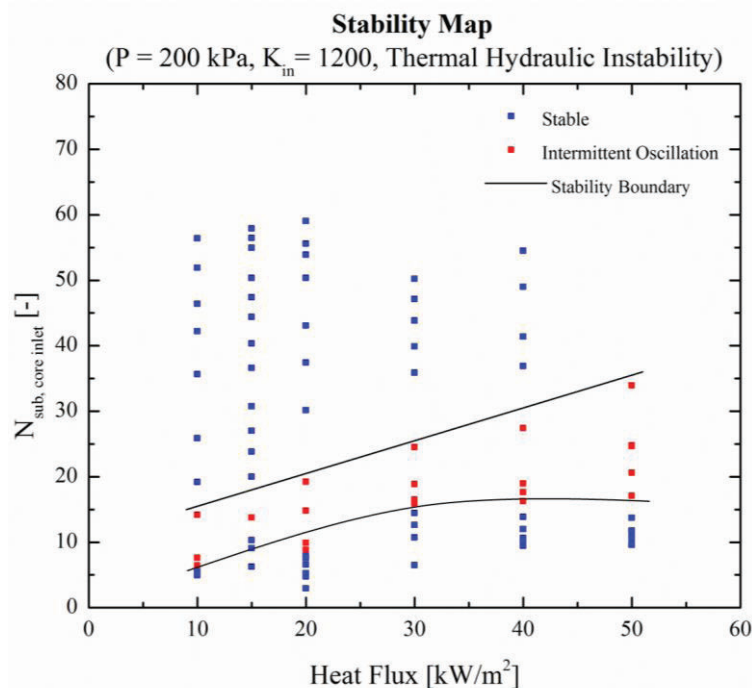
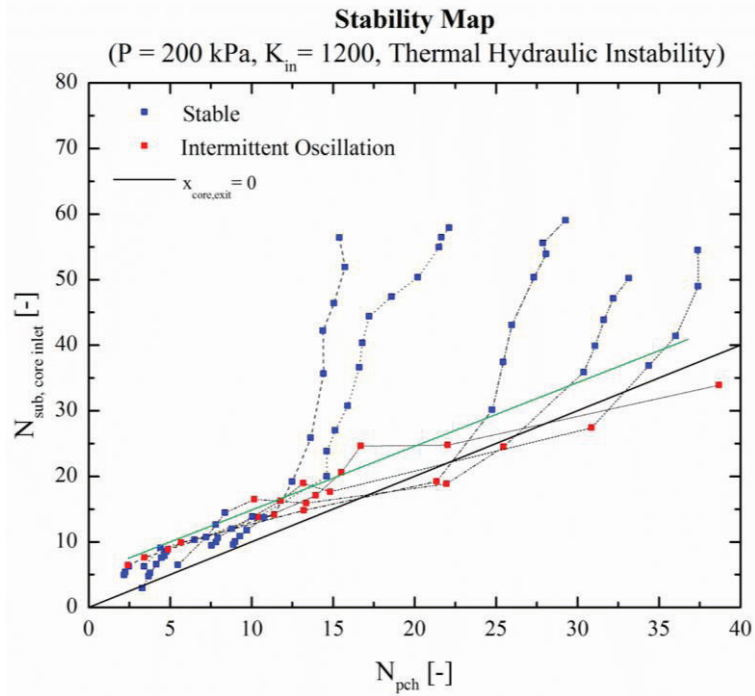


Figure 6. Stability Map at 200 kPa ( $K_{in} = 1200$ )

The same amount of testing points is plotted again in the non-dimensional plane with the zero quality line at the core exit in Fig. 7. From Eq. (3), the subcooling number is equal to the phase change number along the zero quality. In the stability map for 200 kPa, most testing points are located above the zero quality line except few unstable transient points, which means the testing conditions are in the thermal non-equilibrium conditions. The flashing in the chimney due to reduced hydro-static head leads to the intermittent flashing oscillations. At low pressure, the flashing in the chimney plays a major influence on the development of two-phase natural circulation rather than the boiling in the heated section.



**Figure 7. Stability Map in Stability Plane ( $N_{sub}$ - $N_{pch}$ ) at 200 kPa ( $K_{in} = 1200$ )**

If one group of data for certain core flux is carefully investigated, the change of phase change number is not sensitive to the decreasing of subcooling number during the single-phase natural circulation. However, the phase change number reduces substantially when the coolant in the test section starts to boil. The boundary in the green line between the single-phase and the two-phase is clearly shown in the stability map. The two-phase natural circulation testing conditions are in the low phase change number region due to larger natural circulation rate compared to that of single-phase natural circulation rate. The time trace of natural circulation rate at three phases can be seen in Fig. 8. For both single-phase and two-phase natural circulation, the core inlet flow velocities are stable. However, the flow velocity shows a big peak during the transition phase due to the flashing instability. The density wave oscillations observed during the startup transients is not able to be investigated for the following two reasons. First, the density wave oscillations might exist for a very short time, current test strategy cannot determine the unstable density wave oscillations. Secondly, even if density wave oscillations exist, the boundary is hard to plot due to the experimental testing points in the stability map moving to the low subcooling number and phase change number region. In other words, the density wave oscillation is not a dominant instability mechanism at low pressure conditions for natural circulation test facility or reactor.

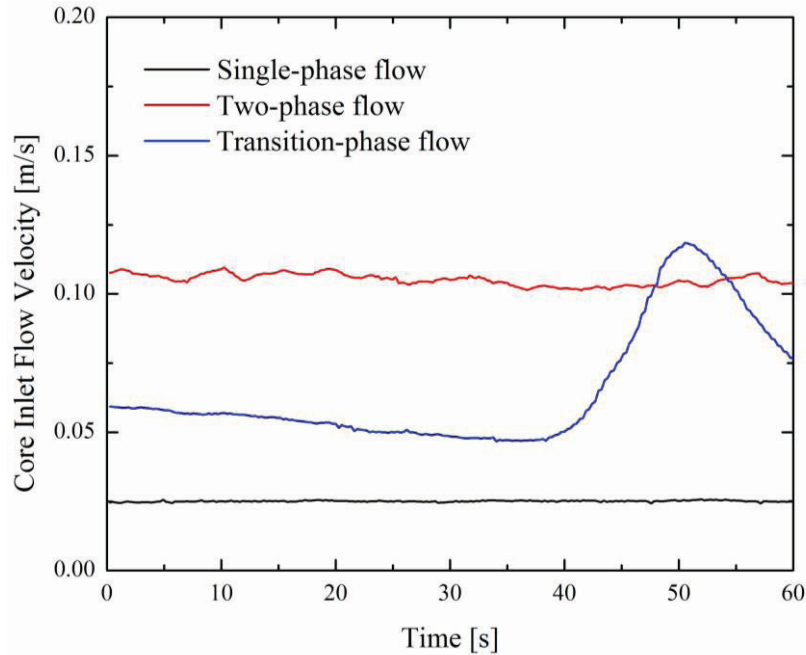


**Figure 8. Core Inlet Flow Velocity Profile at Different Phases**

#### **4.2. Stability Maps at 400 kPa of System Pressure**

The flashing instability is the main flow instability mechanism observed in the quasi-steady tests at the pressure of 200 kPa. In order to investigate the pressure effects on the flow stability, the experimental quasi-steady tests are performed at the pressure of 400 kPa. The testing conditions are plotted in the plane of subcooling number against the core heat flux in Fig.9. The general trend of the stability conditions is quite similar to that of pressure of 200 kPa. Figure 9 shows two boundaries between the stable single-phase and transition phase can be plotted. However, compared to the stability map at the pressure of 200 kPa, single-phase stable region is larger at the pressure of 400 kPa. The boundary between the single-phase region and the transition phase moves downward to the smaller subcooling number. And the unstable region of flashing instability at 400 kPa is smaller than that at 200 kPa by comparing the change of subcooling number between stable testing conditions for a certain heat flux.

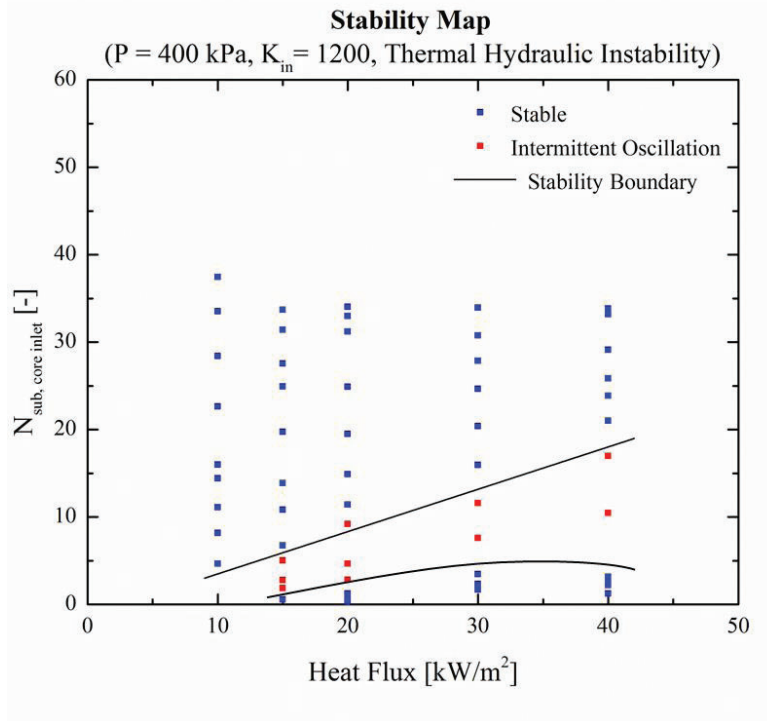


**Figure 9. Stability Map at 400 kPa**

Using the same analysis method, the stability map plotted in the dimensionless plane of  $N_{pch}$ - $N_{sub}$  is presented in Fig. 10. As can be seen, this stability map is similar to the map under 200 kPa. Some abnormal testing points at high subcooling number are caused by unstable operating conditions at the beginning of the test. However, the stability boundary between the single-phase natural circulation and transition phase moves to the zero quality line at the core exit when the system pressure is increased to 400 kPa. In other words, the subcooled boiling is largely reduced at higher pressure, which moves the flashing boundary to the zero quality line calculated in thermal equilibrium conditions. And the unstable region of the transition phase is very thin at this pressure. The stable two-phase testing points moves to the very left-bottom corner in the map. The testing results indicate that the higher pressure can suppress the vapor generation caused by flashing instability in the chimney due to reduced hydrostatic head. So the pressurized startup procedures are used to eliminate the flow instabilities for the startup transients in previous research [7].

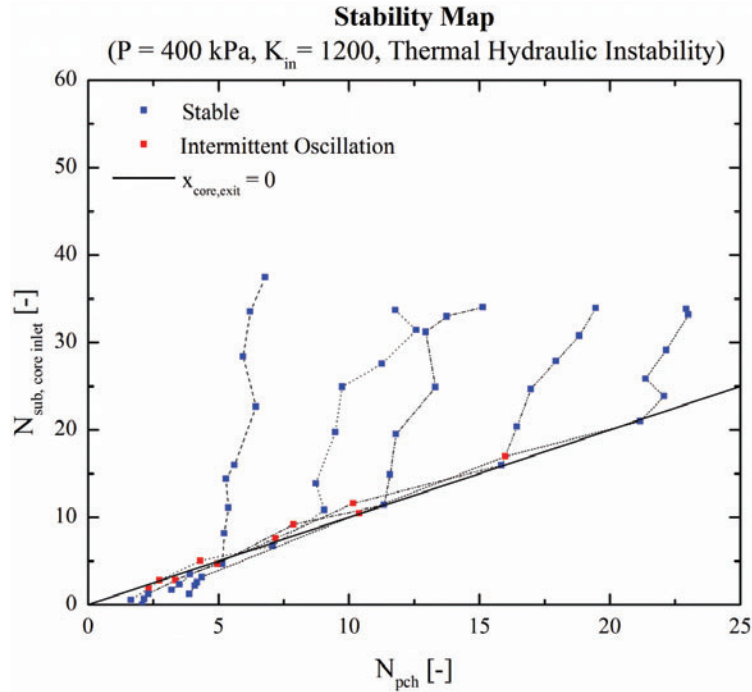


Figure 10. Stability Map in Stability Plane ( $N_{sub}$ - $N_{pch}$ ) at 400 kPa ( $K_{in} = 1200$ )

#### 4.3. Stability Maps for Core-Wide Nuclear Coupling at 400 kPa of System Pressure

The nuclear coupled flow instability by considering void reactivity feedback has been investigated after flow oscillations reported in two commercial BWRs, i.e., Coorso in Italy [8] and LaSalle 2 in USA [9]. In the previous research, the void reactivity feedback was investigated on the flow instability during the startup transients for different power ramp rates. The conclusion is that the void reactivity feedback has trivial effects on the flashing instability during the transition phase. The void reactivity feedback might induce the density wave oscillation (DWO) due to power oscillation during the two-phase natural circulation.

In order to investigate the void reactivity feedback on the stability map, the quasi-steady tests at 400 kPa are performed by considering the void reactivity feedback. The reactivity physics and detailed analysis can be found in the previous research on the startup transients considering the void reactivity feedback [10]. In this section, only the polynomial form of the reactivity change as a function of the void fraction is introduced

$$\Delta\rho(\alpha) = -26.694 - 78.043\alpha - 0.2403\alpha^2 - 3E-05\alpha^3 \quad [\text{pcm}] \quad (7)$$

Figure 11 shows the stability map with non-dimensional plane at 400 kPa with the same other conditions as thermal-hydraulic tests. The void reactivity feedback is considered from the single-phase region, where can have subcooled boiling in the heated section. There are three lines plotted with different core heat flux to show experimental testing matrix. As can be seen, the boundary between the single-phase and two-phase natural circulation is still the line of  $x_{core,exit} = 0$ , which is similar to the stability map without considering the void-reactivity feedback at pressure of 400 kPa. However, big variations in the phase change number can be observed for a fixed heat flux, which means the power oscillations in the single phase region. This stability map confirms that void reactivity feedback can cause the power oscillations

but not the change of the flashing stability boundary. Because the DWO is not easily distinguished during the quasi-steady tests, the stability boundary for density wave oscillation considering the void reactivity feedback is not presented in this paper.

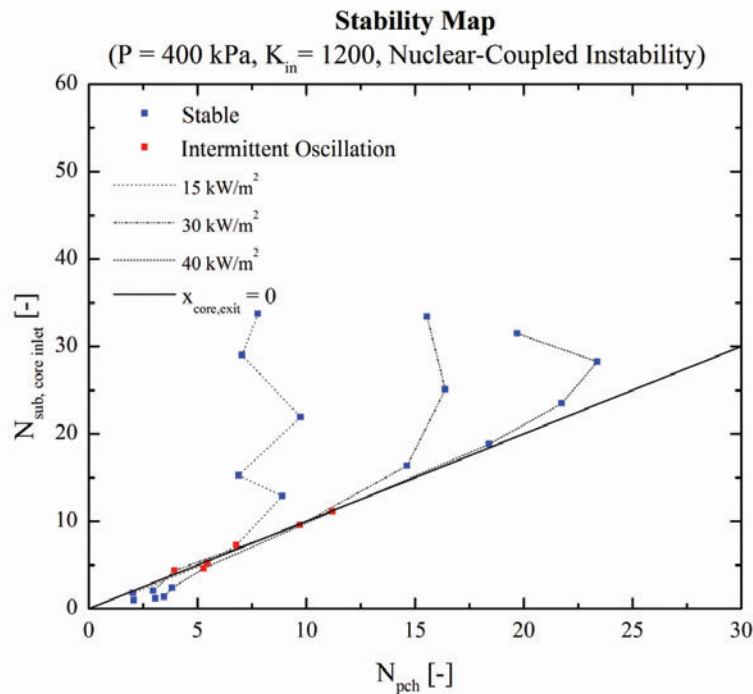


Figure 11. Stability Map in Stability Plane ( $N_{sub}$ - $N_{pch}$ ) with Nuclear-Coupling at 400 kPa

## 5. CONCLUSIONS

Following previous startup transient tests for the NMR, low pressure quasi-steady tests were performed in a well-scaled BWR-type natural circulation test facility to understand the mechanism of flow instabilities in the startup transients. The stability maps were generated in the dimensionless plane of  $N_{sub}$ - $N_{pch}$  at the core inlet pressure of 200 kPa and 400 kPa. The quasi-steady tests cover experimental conditions from single-phase natural circulation to two-phase natural circulation.

The flashing instability is the main flow instability observed during the tests at different system pressure. The flashing stability boundary can be drawn between the single-phase stable conditions and two-phase stable conditions in the stability plane. The stability boundary at the 200 kPa is above the line of zero quality line at the core exit, while the boundary moves to the zero quality line at the pressure of 400 kPa. So the flashing instability at low pressure less than 400 kPa is mainly caused by the thermal non-equilibrium vaporization due to reduced hydrodynamic head in the chimney. Furthermore, the void reactivity feedback is simply investigated in current research. The results show that the void reactivity feedback does not have big influence on the boundary of the flashing stability except for the power oscillations in the stable region. In the future, the experimental stability maps are going to be used to benchmark the numerical frequency domain analysis of the stability boundary for the NMR.

## NOMENCLATURE

### Latin Letters

$K_{in}$	Inlet flow orifice coefficient (-)
$\dot{m}_o$	Mass flow rate (kg/s)
$n$	Sample size (-)
$N_{sub}$	Subcooling number (-)
$N_{pch}$	Phase change (Zuber) number (-)
$P$	Pressure (Pa)
$\dot{Q}$	Total heat transfer rate (W)
$v_{in}$	Inlet velocity (m/s)
$x_e$	Vapor quality at the core exit (-)

### Greek Letters

$\alpha$	Void fraction (-)
$\lambda^*$	Non-boiling length (-)
$\Delta$	Difference (-)
$\Delta i_{fg}$	Latent heat (J/kg)
$\Delta i_{sub}$	Subcooling in terms of enthalpy (J/kg)
$\rho_g$	Gas density (kg/m <sup>3</sup> )
$\Delta\rho$	Reactivity change (-)
	Density difference (kg/m <sup>3</sup> )

## ACKNOWLEDGMENTS

This material is based upon work supported under a Department of Energy Nuclear Energy University Program.

## REFERENCES

1. G. N. Energy, "SBWR standard safety analysis report," Rep. 25A5113 Revd. A (1992).
2. M. Ishii, T. Hibiki, W. S. Yang, J. Schlegel, Z. Wu, S. Shi, Y. Lin, J. H. Eoh, C. S. Brooks, and C. Clark, "Investigation of Natural Circulation Instability and Transients in Passively Safe Small Modular Reactors - Annual Report," PU/NE-13-10 (2013).
3. M. Ishii, T. Hibiki, W. S. Yang, J. Schlegel, Z. Wu, S. Shi, Y. Lin, J. H. Eoh, Z. Liu, and C. Clark, "Investigation of Natural Circulation Instability and Transients in Passively Safe Small Modular Reactors - Startup Transient Analysis of NMR-50 for Scaled BWR Experimental Facility," PU/NE-14-04 (2014).
4. M. Ishii, "Thermally induced flow instabilities in two-phase mixtures in thermal equilibrium," Dissertation, Georgia Institute of Technology (1971).
5. M. Ishii, S. T. Ravankar, and R. Dowlati, "Scientific design of Purdue University Multi-Dimensional Integral Test Assembly (PUMA) for GE SBWR," (1996).
6. A. Dixit, T. Hibiki, M. Ishii, K. Tanimoto, Y. Kondoh, and K. Hibi, "Start-up transient test simulation with and without void-reactivity feedback for a two-phase natural circulation reactor," Nucl. Eng. Des., **265**, pp. 1131-1147 (2013).
7. S. Shi, C. Brooks, J. Eoh, and M. Ishii, "Pressurized Startup Transient Analyses for the BWR-type NMR-50," presented at the American Nuclear Society Winter Meeting, Anaheim, CA, USA (2014).

8. Gialdi, E., Grifoni, S., Parmeggiani, C., Tricoli, C., "Core stability in operating BWR: operational experience," Prog. Nucl. Energy, Fourth Specialists Meeting on Reactor Noise, **15**, pp. 447-459 (1985).
9. US NRC, "Power oscillations in boiling water reactors (No. NRC bulletin 88-07)," (1988).
10. S. Shi, F. Odeh, M. Ishii, W. S. Yang, Y. Yan, and Y. Lin, "Investigation of Natural Circulation Instability and Transients in Passively Safe Small Modular Reactors - 2014 Annual Report," PU-NE-14-08, (2014).